JOURNAL OF PROPULSION AND POWER
Vol. 9, No. 3, May–June 1993

Anode Power Deposition in Magnetoplasmadynamic Thrusters

A. D. Gallimore,* A. J. Kelly,† and R. G. Jahn‡
Princeton University, Princeton, New Jersey 08544

Results of anode heat-flux and anode fall measurements from a multimegawatt self-field quasisteady magnetoplasmadynamic (MPD) thruster are presented. Measurements were obtained with argon and helium propellants for a variety of currents and mass flow rates. Anode heat flux was directly measured with thermocouples attached to the inner surface of a hollowed section. Anode falls were determined both from floating probes and through heat flux measurements. Comparison of data acquired through either method shows excellent agreement. Anode falls varied between 4–50 V with anode power fractions reaching 70% with helium at 150 kW, and 50% with argon at 1.9 MW. The anode fall was found to correlate well with electron Hall parameters calculated from triple Langmuir and magnetic probe data collected near the anode. Two possible explanations for this result are proposed: 1) the establishment of large electric fields at the anode to maintain current conduction across the strong magnetic fields; and 2) anomalous resistivity resulting from the onset of microturbulence in the plasma. To investigate the latter hypothesis, electric field, magnetic field, and current density profiles measured in the vicinity of the anode were incorporated into Ohm's law to estimate the electrical conductivity. Results of this analysis show a substantial deviation of the measured conductivity from that calculated with classical formulas. These results imply that anomalous effects are present in the plasma near the anode.

Nomenclature

B = magnetic field strength, T
E = electric field, V/m
e = elementary charge, 1.6×10^{-19} C
J = thruster current, kA
J_a = total anode current, A
j = current density, A/cm^2
j_a = anode current density, A/cm^2
k = Boltzmann's constant, 1.38×10^{-23} J/K
$\dot{m}$ = propellant mass flow rate, g/s
$\dot{m}_e$ = propellant mass flow rate, g/s
n_e = electron number density, m^{-3}
P_t = total anode power, W
p_e = electron pressure, Pa
$\dot{q}_a$ = anode heat flux, W/cm^2
$\dot{q}_c$ = anode heat flux from convection, W/cm^2
$\dot{q}_r$ = anode heat flux from radiation, W/cm^2
T = thrust, N
T_e = electron temperature, K
T_i = ion temperature, K
V = terminal voltage, V
V_a = anode fall, V
v = plasma streaming velocity, m/s
ε_0 = permittivity of free space, 8.85×10^{-12} F/m
η_a = anode power fraction
$\eta_\perp$ = transverse electrical resistivity, Ohm-m
Λ = plasma parameter
λ_e = Debye length, m
ν_e = electron collision frequency, s^{-1}
σ_{sh} = Spitzer-Härm conductivity, mho/m
σ_0 = inferred electrical conductivity, mho/m
ϕ = anode material work function, 4.62 V
Ω = Hall parameter
Ω = inferred Hall parameter
Ω_{sh} = classically calculated Hall parameter
ω_e = electron gyrofrequency, rad/s

Received March 23, 1992; revision received Oct. 14, 1992; accepted for publication Nov. 23, 1992.

*Graduate Assistant, Electric Propulsion Laboratory, Department of Mechanical and Aerospace Engineering; currently Assistant Professor, Department of Aerospace Engineering, University of Michigan, Ann Arbor, MI 41809. Member AIAA.

†Manager and Senior Research Engineer, Electric Propulsion Laboratory. Member AIAA.

‡Professor, Electric Propulsion Laboratory, Department of Mechanical and Aerospace Engineering. Fellow AIAA.

Introduction

WITH high specific impulse and simple design, the MPD thruster is an attractive candidate for propulsion applications ranging from Earth orbit payload raising to manned and unmanned planetary missions.[1,2] The utility of the device as a primary means of space propulsion, however, is severely limited by its low efficiency.[3–6] The two loss mechanisms responsible for limiting thruster efficiency are frozen-flow loss, which is the dominant loss mechanism for thruster power levels above 1 MW, and anode power dissipation, which is especially detrimental to thrusters operating at submegawatt power levels. At thruster power levels below 150 kW, over half of the input power can be deposited into the anode.[4,6] While the fraction of total power deposited into the anode decreases with thruster power, the magnitude of the heat flux to the anode [O(10 kW/cm^2)] poses a serious thermal management problem to spacecraft designers. An understanding of the physical processes involved in anode power deposition is essential for the design of efficient engines. The complexity of the processes involved and lack of a theoretical model necessitates careful experimentation for insight.

For reasons that will become apparent below, most experimental research in anode power dissipation has focused on understanding how the anode fall is influenced by plasma and thruster operating conditions. Studies have shown that the anode fall tends to decrease with increasing local curent density,[3,5,7,8] while others have shown negative fall voltages are present when the local random electron flux to the anode is greater than that required for current continuity.[9,10] However, no universal scaling parameter for the anode fall has emerged and a detailed understanding of the physics involved with anode power deposition has yet to be established. The goal of this article is to identify key scaling parameters of the anode fall as well as the possible underlying physical processes that control it.

Experimental Facility

A Plexiglas® vacuum tank 1.83-m long with an inner diameter of 0.92 m was used for these experiments. Tank pres-

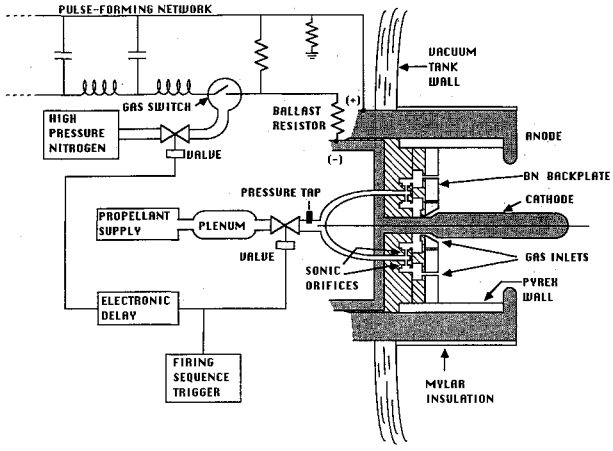

Fig. 1 Quasisteady MPD thruster apparatus.

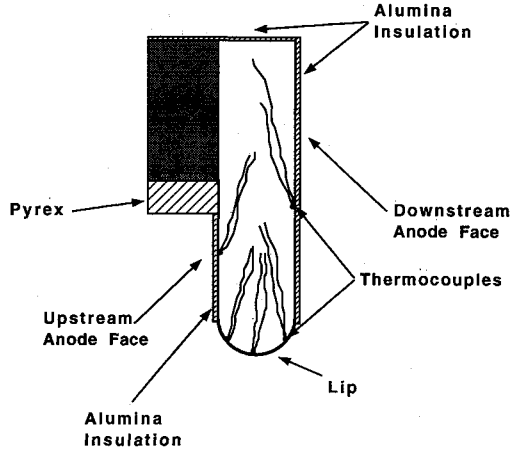

Fig. 2 Cross-sectional view of anode shell.

sure was maintained to less than 0.02 Pa (1×10^{-4} Torr) prior to thruster operation by a 15-cm oil diffusion pump and two mechanical backing pumps. The tank contains an electronically controlled probe positioning table with three degrees of freedom (DOF) as well as angular freedom in the horizontal plane. Thruster power is supplied by a 160-kJ pulse-forming network (capacitor bank) capable of delivering a rectangular current pulse of up to 52 kA for 1 ms (cf. Fig. 1).

The thruster used for these experiments consists of an aluminum cylindrical thrust chamber 5-cm deep with an i.d. of 15 cm and an o.d. of 19 cm. The inner surface of the thrust chamber is insulated from the discharge by a Pyrex® tube with a wall thickness of ~1 cm. The cathode, made of 2% thoriated tungsten, is 10-cm long and 1.8 cm in diameter. Propellant is injected through the boron-nitride backplate by way of 12 3-mm-diam holes at a radius of 3.8 cm, and through an annulus at the base of the cathode. An equal amount of propellant flows through the holes and the annulus. The anode consists of a 1-cm-thick aluminum ring of o.d. 19 cm and with an i.d. of 10 cm. A section of the anode was hollowed to form a cavity with a wall thickness of 1 mm. Copper-constantan thermocouples (no. 36 gauge) were attached to the inner wall of the cavity with a thermally conductive epoxy. To investigate what effect current density has on anode power deposition, a 0.13-mm-thick (5-mil) layer of alumina was plasma-sprayed over 85% of the anode's surface area, exposing only the lip to the discharge (cf. Fig. 2). Alumina was selected in order to minimize the amount of contaminant material released to the plasma from insulator ablation. The remaining outer surface of the thruster was insulated with mylar tape.

Diagnostics

The fraction of thruster power consumed by the anode may be written as[11]

$$\eta_a \equiv \frac{P_t}{VJ_a} = \frac{1}{VJ_a} \oint_S \dot{q}_a \cdot \mathrm{d}S \tag{1}$$

where the integration is performed over the entire current conducting surface of the anode. The integrand of Eq. (1) defined by

$$\dot{q}_a = j_a [V_a + (5/2)(kT_e/e) + \phi] + \dot{q}_c + \dot{q}_r \tag{2}$$

represents the contribution to anode heating from the kinetic energy that current carrying electrons gain from the anode fall, the random electron thermal energy, the heat liberated due to the work function of the anode material, and contributions from plasma convection and radiation. Anode heating from convection and radiation has been estimated to be negligible for high-powered quasisteady thrusters, where the total anode heat flux can exceed several kilowatts per square centimeter.[5,7,12,13] Furthermore, for typical operating conditions, the contribution to anode heating from the anode fall, which can exceed 20 V, is much greater than those due to electron random thermal energy (1–4 eV), or the work function (<5 eV). Therefore, understanding the underlying physics of the anode fall is necessary for the reduction of losses to the anode.

To further investigate previous findings, that reducing the conducting surface area of the anode leads to a substantial decrease in the terminal voltage and anode fall,[5,8] the "standard" bench mark thruster was compared to a similar thruster with the coated anode ("modified" bench mark thruster). Initial tests revealed that the voltage-current characteristic of the two engines are almost identical, indicating that in contrast to the trends shown in previous work (Ref. 8), the reduction of the anode current conduction area, by a factor of 6, has little impact on the voltage-current characteristics of the thruster.

To investigate the influence of anode surface area (current density) on anode power deposition, a one-dimensional heat conduction model[3] is used to infer incident anode heat fluxes from the temperature response of the imbedded thermocouples (cf. Fig. 2). Special thermocouples, capable of measuring temperatures with accuracies of ±0.5°C, limited the error in heat flux measurements due to thermocouple temperature response to ~130 W/cm².[3] Thermocouple signals were processed by a personal computer through a Keithley System 570 data acquisition system. The thermocouples were attached to the anode shell with a special epoxy (Omegabond® 200) that was selected for its high thermal conductivity and high electrical resisitivity (to protect the computer from the high-voltage start-up pulse). During each thruster firing, the Keithley system sampled two temperature measurements per thermocouple. The first measurement is made before the heat from the plasma has had time to conduct through the shell (~1 ms after the initiation of propellant breakdown). The other measurement is taken 20 ms later, when the thermocouple temperature rise was experimentally determined to have plateaued to its maximum value.[3]

Figure 3 shows anode heat flux measurements from thermocouple data as a function of position along the anode shell for both the standard and modified bench mark thrusters. The abscissa of the figure represents a coordinate that linearly maps onto the surface of the anode, the extreme left (−2.0 cm) and right (4.0 cm) ends of the plot representing the extent of the upstream and downstream faces of the anode, respectively. As the figure shows, the peak heat flux is on the order of several kilowatts per square centimeter, while heat fluxes for the two thermocouples located behind the insulation are generally an order of magnitude less. The response of the thermocouples at the insulated sites is due to both transverse

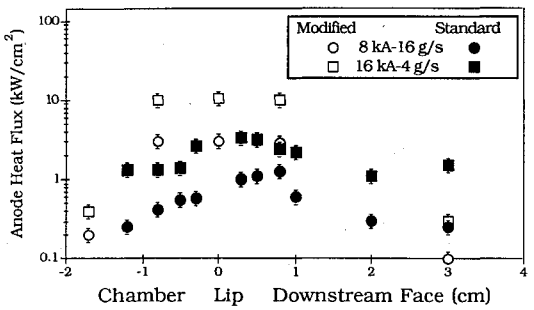

Fig. 3 Anode heat flux vs thermocouple position.

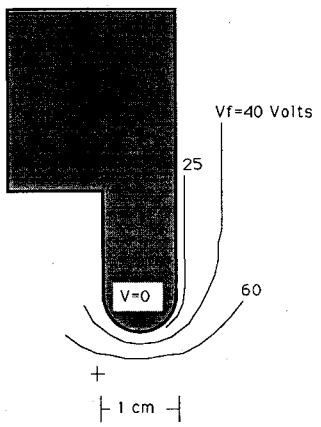

a) Standard bench mark thruster

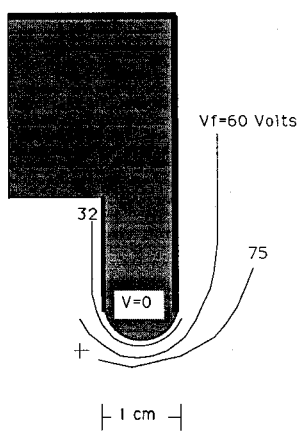

b) Modified bench mark thruster

Fig. 4 Floating potential profiles (16 kA and 4 g/s).

heat conduction along the shell and heating from the ambient plasma.

Floating probe measurements of the anode fall were conducted as a second means of estimating anode power deposition. The probe was shaped in the form of an "L" to enable probing along the upstream anode face. The probe has a 54-cm major arm and a 1.4-cm minor arm which supports a tungsten wire electrode that is 0.026 cm (10 mil) in diameter and 0.17-cm (65-mil) long. Details of the apparatus for the floating probe measurements are described in Ref. 14.

Figure 4 shows equipotential profiles near the anode of the standard and modified bench mark thrusters at 16 kA and 4 g/s. In general, as is evident from the figure, the gradient of floating potential for the modified bench mark thruster is larger than that of the standard thruster. This reflects the response of the plasma to the increased local current density. For both thrusters, the region of intense floating potential gradients extends up to 1 cm from the anode surface.

A triple Langmuir probe was employed to measure electron temperatures that are needed both to convert floating potentials to actual plasma potentials and for the estimate of the anode fall from the measured heat flux [Eq. (2)]. A description of the triple probe system and data reduction algorithm used for these experiments are presented in Refs. 3, 15–17. Electron temperatures and ion number density measurements are accurate to within 10 and 60%, respectively.[17]

Figure 5 shows the "mean" anode falls obtained from both heat flux measurements (part a) and from the floating probe measurements taken 1 mm from the anode surface (part b), the closest distance permissible with the probe positioning system. To obtain the mean fall values, anode falls for each thermocouple or floating probe measurement site were weighted by the local current density. By entering the average anode fall into Eqs. (1) and (2), neglecting convection and radiation, the total measured power to the anode is recovered. Anode fall estimated from heat flux measurements are accurate to within 30 and 15% for the standard and modified bench mark thrusters, respectively. The difference in error of the two thrusters is due to the large error (50%) associated with the extrapolated current density profiles of the standard bench mark thruster.[3] Because current conduction is restricted to a small portion of the modified bench mark thruster, a constant current density can be assumed at each of the appropriate thermocouple sites. Floating probe measurements are accurate to within ±2 V.

The figure illustrates two important points: 1) there is little difference between the mean anode falls (at 1 mm) of either thruster; and 2) that anode fall values from thermocouple and floating probe data are in agreement with each other, except at the highest thruster exhaust velocity ($J^2/\dot{m}$). This discrepancy had at one time been attributed solely to ablation of the anode surface material, resulting in an energy sink not accounted for in the heat conduction model. As will be shown below, however, some of this disagreement may also be due simply to a voltage drop through the highly resistive plasma near the anode.

The figures in this section have shown that the reduction of anode surface area has minimal effect on the operating characteristics of the MPD thruster. The failure of this ex-

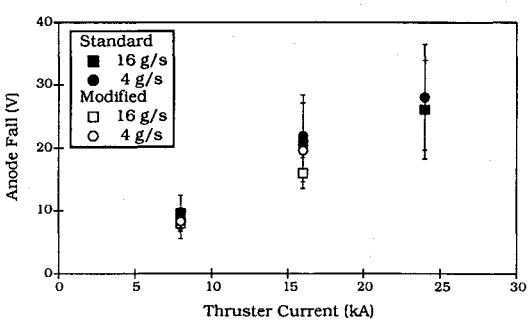

a) Thermocouple

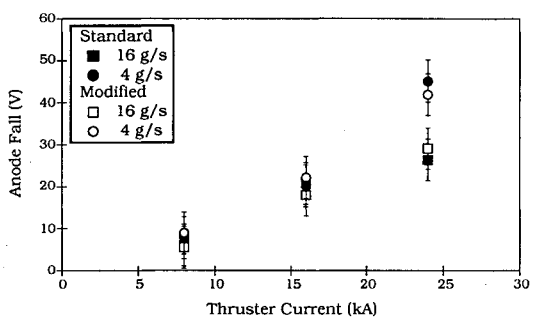

b) Floating probe

Fig. 5 Anode fall vs thruster current.

periment to reproduce the results reported in Refs. 5 and 8 may be attributed to the following factors:

1) The reduction of the anode surface area may not have been enough. The anode used in Ref. 8 reduced the conduction area by a factor of 40 by limiting current conduction to a 2-mm band around the anode lip.

2) The mylar tape used to insulate 98% of the anode surface in Ref. 8 may have ablated, introducing mass to the local plasma. (Inspection of the tape later showed that a substantial portion of it was missing, presumably due to ablation.)

Anode Fall Measurements

The anode falls determined through direct heat-flux measurements are in general agreement with those determined with floating probes. Since floating probes are considerably simpler to implement than the heat-flux apparatus, a series of floating probe measurements of the anode fall was made to establish trends in anode power deposition. The floating electrode of the triple probe was used to measure the plasma's floating potential 1 mm from the anode surface, with the length of the probe electrodes placed in the plane of the anode lip. Floating potentials were converted to the plasma potentials with the electron temperatures measured by the triple probe; allowing for the instantaneous measurement of plasma potential. The L-shaped floating probe was also employed in several anode fall measurements at the lip. The floating potentials measured with the triple probe agree to within 5% of those obtained with the floating probe.

This series of experiments was carried out on the modified bench mark thruster with argon propellant at mass flow rates of 4, 6, 8, 12, and 16 g/s at thruster currents between 4 and 25 kA, and with helium propellant at mass flow rates of 1, 2, 4, and 6 g/s at thruster currents between 4–22 kA. These conditions correspond to a range of $J^2/\dot{m}$ between 1–160 kA^{2}s/g for argon, and 3–400 kA^{2}s/g for helium. Thruster power varied between 150 kW and 7 MW for argon, and from 150 kW to 3.5 MW for helium.

Figure 6 shows the anode fall as a function of thruster current for argon and helium at various mass flow rates. For both propellants, the anode fall ranged from 5 to 50 V. The larger error bars of the helium data signify the relative scatter in measured data; scatter that is not exhibited by the argon data. With argon propellant, the anode fall increases monotonically with current between 4–16 kA and is independent of mass flow rate. Above 16 kA, the anode fall is strongly dependent on mass flow rate, rising steeply with thruster current. The helium data, however, exhibit less coherence with propellant flow rate. Although the lowest anode falls were measured at the highest mass flow rates (6 g/s), anode falls measured at relatively large flow rates (4 g/s) are almost as large as those measured at much lower rates for identical currents.

Figure 7 shows the anode fall as a function of $J^2/\dot{m}$ for argon and helium propellants. As was observed in a previous study with argon propellant,[9] there is a strong increase in the anode fall with $J^2/\dot{m}$. However, unlike the study of Ref. 9, which was limited to a maximum $J^2/\dot{m}$ of 30 kA^{2}s/g, beyond a certain value (70 kA^{2}s/g) the anode fall remains constant. For helium, below a $J^2/\dot{m}$ of 100 kA^{2}s/g there is a great deal of scatter in the data, with little dependence on mass flow rate. Above this value, the anode fall increases monotonically with $J^2/\dot{m}$, in sharp contrast to the behavior displayed by the argon data which plateaued above 70 kA^{2}s/g. It is possible that, for helium, the asymptotic dependence of the anode fall is reached only at much higher values of $J^2/\dot{m}$.

Equations (1) and (2) were used with anode fall and electron temperature data to estimate the fraction of thruster power deposited to the anode. For all calculations, convection and radiation are neglected. Figure 8 shows anode power fraction as a function of total thruster power. As part a of the figure clearly illustrates, anode power fraction is heavily dependent on mass flow rate. The anode power fraction varies from 0.5 at 1.9 MW (12 g/s), to 0.23 at 7 MW (4 g/s). Below a power level of 2.5 MW, substantial scatter for the different mass flow rates is present. Above this value, however, anode power fraction decreases monotonically with increasing thruster power.

In Fig. 8b anode power fraction for helium propellant is shown as a function of thruster power. In general, because of lower terminal voltages, the anode power fractions with

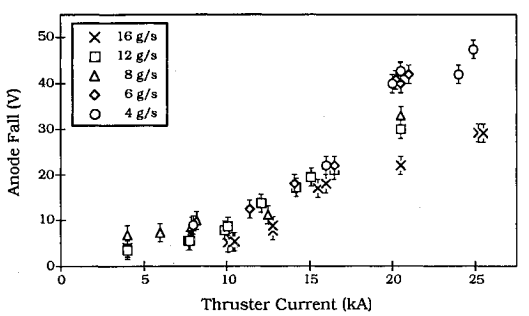

a) Argon

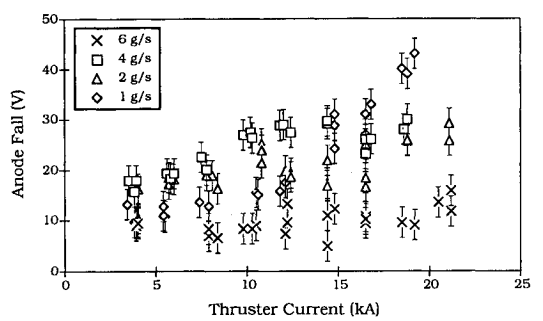

b) Helium

Fig. 6 Anode fall vs thruster current.

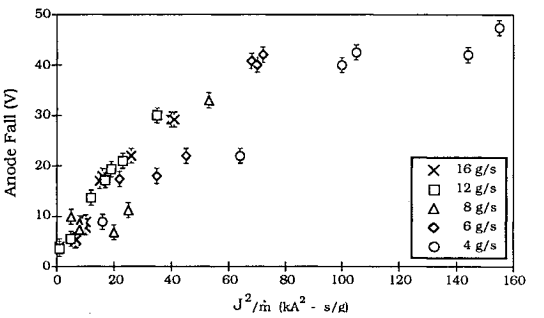

a) Argon

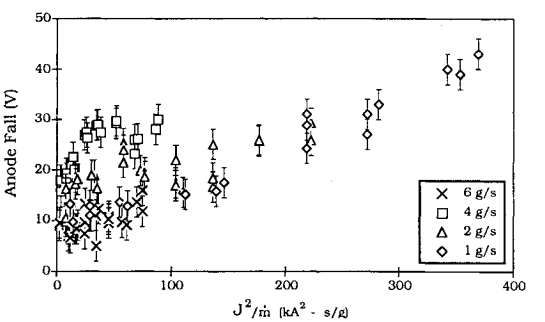

b) Helium

Fig. 7 Anode fall vs $J^2/\dot{m}$.

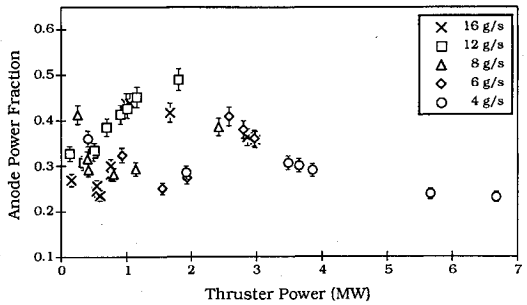

a) Argon

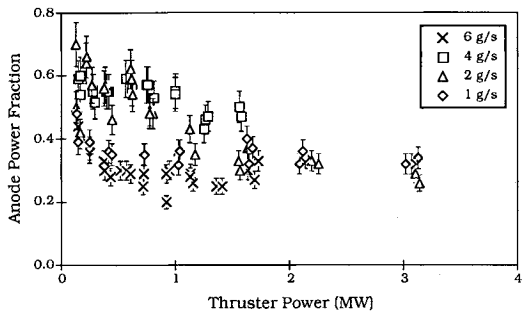

b) Helium

Fig. 8 Anode power fraction vs thruster power

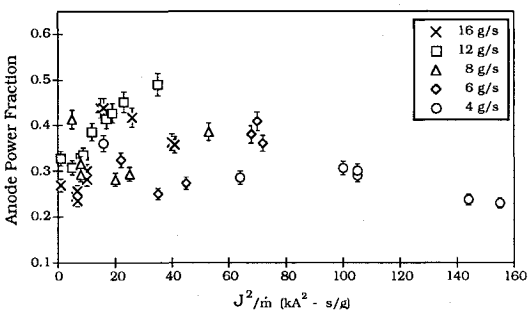

a) Argon

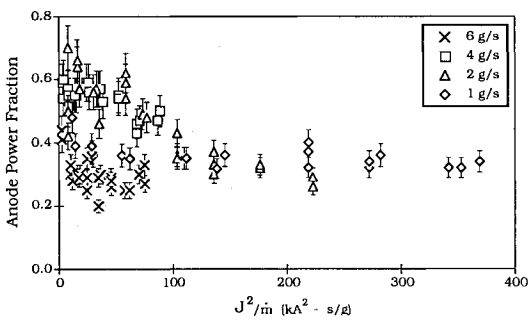

b) Helium

Fig. 9 Anode power fraction vs $J^2/\dot{m}$.

helium propellant at a given thruster power level (or $J^2/\dot{m}$) are larger than those with argon. The anode power fraction ranges from 0.7 at 150 kW (2 g/s) to 0.25 at 3.2 MW (2 g/s). Again, the data exhibit little dependence on mass flow rate, particularly at the submegawatt power levels. At submegawatt levels, relatively high propellant flow rates can yield either large or small values of anode power fraction at a given level of thruster power. Since power fraction is linked to the terminal voltage characteristics, much of this behavior is a direct result of the dependence of the resistive (and back emf) voltage drop through the plasma on thruster operating conditions.

Figure 9 shows anode power fraction as a function of $J^2/\dot{m}$ for argon and helium propellants. For argon, above a $J^2/\dot{m}$ of 70 kA²s/g, the anode power fraction decreases with increasing $J^2/\dot{m}$, reflecting the constant value of the anode fall within this range. For helium, however, above a $J^2/\dot{m}$ of 100 kA²s/g, the same range in which the anode fall monotonically increases with $J^2/\dot{m}$, the anode power fraction remains constant. Below these specific values of $J^2/\dot{m}$ the anode power fraction is again highly dependent on propellant mass flow rate.

Anode Fall Scaling Parameter

Much effort in the past has been dedicated to the identification of scaling parameters for the anode fall.[3-10] Some of this work has linked sizable voltage drops at the anode to large electron Hall parameters in the adjacent plasma. Anode voltage drops of 20–50 V in an atmospheric pressure magnetohydrodynamic (MHD) accelerator/generator correlated well with calculated electron Hall parameters.[18] This trend has been observed with multimegawatt pulsed plasma injectors operating at significantly less pressure (~10 Torr) as well.[19] Although several mechanisms have been evoked to explain large anode falls, including anode starvation,[10,20] whereby large electric fields are established at the anode in response to the depletion of charge carriers by means of electromagnetic pumping,[21] and anomalous resistivity resulting from plasma microturbulence,[22-25] no definitive theoretical or experimental work linking the Hall parameter to anode power deposition in MPD thrusters exists. In an effort to investigate this behavior, the triple and floating probe data described above, in conjunction with a series of magnetic field measurements taken at the anode lip, were employed to obtain an estimate of the local electron Hall parameter.

The electron Hall parameter is defined as the ratio of the electron gyrofrequency to the electron-ion collision frequency. In order to calculate both of these quantities, the electron temperature, number density, and the local magnetic field must be measured. A magnetic field probe (B probe), originally constructed to investigate asymmetries in the thruster discharge,[26] was used for this experiment. The core of the probe consists of a coil with 30 turns of no. 44 Formvar®-coated copper wire on a 1.5-mm-diam Lucite® rod. The core and probe signal lines are enclosed in a quartz tube 61-cm long with an o.d. of 4 mm. One end of the quartz tube terminates to form a hemisphere for protection of the core. The axis of the core was aligned with the azimuthal magnetic field lines at a distance of approximately 3 mm from the anode surface. Magnetic probe signals are accurate to within 2%.[26] Details of the construction and calibration of the probe can be found in Ref. 26.

Figure 10 shows the anode fall as a function of Hall parameter for both argon and helium propellants. To calculate the Hall parameter, classical Coulomb collision frequencies (the Spitzer-Härm formula) obtained from triple probe measurements were used in conjunction with measured magnetic fields. The accuracy of the calculated Hall parameter is therefore limited by that of the number density measurements (~60%). As the figure shows, both argon and helium data scale reasonably well with the Hall parameter, in complete agreement with the work of Ref. 18. Note also that the correlation with Hall parameter holds, irrespective of mass flow rate. The calculated Hall parameter ranges from 2 to 10, implying the presence of large axial currents as well as large Hall fields. Due to the large gradient in number density at the anode, however, the Hall parameter just at the surface ($<<1$ mm) may be significantly larger.

Two possibilities which could explain the connection between the anode fall and the Hall parameter exist at this time. One is that large electric fields (parallel and perpendicular to the anode surface), generated by the cross field axial current, may account for the large voltage drops seen at the anode. The electrons are essentially tied to the magnetic field lines and are therefore inhibited from reaching the anode. This

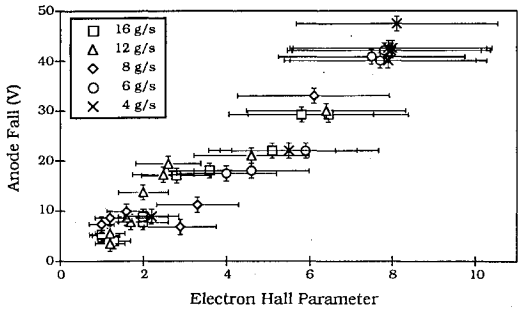

a) Argon

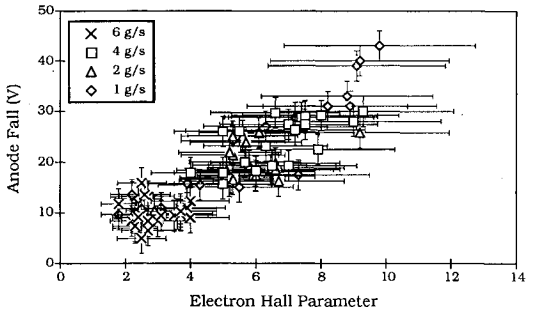

b) Helium

Fig. 10 Anode fall vs electron Hall parameter.

results in the development of a thin layer (on the order of one electron gyro radius ~0.1 mm) of space charge just above the anode surface and large electric fields necessary for current continuity.[19,20]

Alternatively, anomalous electrical resistivity due to plasma microturbulence may be responsible. Excited waves in the plasma scatter current carrying electrons, resulting in an anomalously large collision frequency. As such, large electric fields are needed to maintain current conduction to the anode. The characteristic length scale for such a disturbance, if one exists at all, is not as obvious as for the previous scenario. Therefore, the role of plasma turbulence, which is thought to globally affect thruster operation, in anode power dissipation (i.e., the microscopic anode fall) is unclear. It should be pointed out that on the basis of these experiments there is no direct evidence that the anode fall is the result of a collisionless sheath. Therefore, the measured anode falls (~1-mm away from the surface) may be due to phenomena which can be addressed in the continuum framework.

The question of whether the dissipation of thruster power to the anode is due to phenomena in a collisionless sheath or the continuum plasma (anomalous effects?) is still open to debate. Recently, Choueiri[27] has predicted that a strong correlation exists between anomalous resistivity, due to turbulence in the plasma, and the electron Hall parameter. In the following section, Ohm's law is applied to thruster field (magnetic and electric) and current density measurements to estimate the plasma conductivity.

Inferred Electrical Conductivity

The question of whether anomalous effects play a significant role in the dissipation of power near the anode is still open to debate. For many years, researchers in the USSR have concluded that large electric fields found near the anode are a result of plasma turbulence.[20,22-25] In non-Soviet literature, attempts to link dissipation of thruster power to turbulence have been scarce, with much of this work focused on identifying plasma instabilities through the analysis of terminal voltage[28-30] or Langmuir probe data.[27,31] Although these experiments have demonstrated that instabilities exist in the plasma of MPD thrusters at power ranges that span two orders of magnitude, very little direct measurement of anomalous transport properties (e.g., electrical conductivity) has taken place. Until recently, such measurements were limited to the results of Lovberg[32] in which the electrical resistivity of the plasma in an applied-field quasisteady MPD thruster was inferred from direct measurements of the local electric and magnetic fields, and current density. When compared to the resistivity predicted by classical formulas, it was found that the inferred resistivity was several times (4.0 ± 1.5) that predicted classically. Lovberg[32] concluded that this discrepancy was caused by "collective plasma phenomena" (plasma instabilities).

None of the experimental work described above, however, focused on studying anomalous effects at the anode. The goal of this work was to estimate the plasma electrical conductivity in the anode region of a bench mark MPD thruster through an analysis similar in approach to that of Lovberg. Figure 11 shows a diagram of the MPD thruster as well as the Cartesian coordinate system used for the analysis. Field (magnetic and electric) and current density measurements were made in a standard bench mark thruster operating with argon as propellant. The thruster was operated at 8, 16, and 24 kA at mass flow rates of 4 and 16 g/s. This corresponds to thruster power levels between 300 kW and 7 MW.

We begin the analysis by first writing a form of the generalized Ohm's law suitable for our purpose[37]

$$j = \sigma_0(E + v \times B) - (\Omega/|B|)(j \times B - \nabla p_e) \quad (3)$$

For conditions of interest ∇p_e has been shown experimentally to be negligible in the above equation.[33] The azimuthal current-induced magnetic field (B) defines the z axis of the Cartesian coordinate system (cf. Fig. 11). An axisymmetric current discharge is assumed, allowing for the "z" components of E, v, and j to be neglected. After some algebra we arrive at two equations

$$\sigma_0 = \frac{(1 + \Omega^2)j_x}{(E_x + B_z v_y) + \Omega(B_z v_x - E_y)} \quad (4)$$

$$\sigma_0 = \frac{(1 - \Omega^2)j_y}{\Omega(E_x + B_z v_y) + E_y - B_z v_x} \quad (5)$$

which relate electrical conductivity to "x" and "y" components of current. Only one of these equations is necessary for the analysis. Since j_y represents anode current density, a quantity which has been measured,[34] Eq. (5) is used to calculate σ_0. [Actually, both j_x and j_y were measured. Use of Eq. (4) does not alter the results presented here.] Since σ_0, as defined by the following equation:

$$\sigma_0 = (n_e e^2/m_e \nu_e) \quad (6)$$

is a function of the electron collision frequency, which itself is used to calculate the Hall parameter, an iterative solving

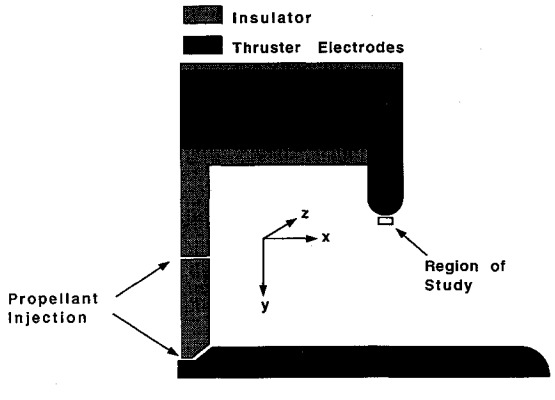

Fig. 11 Cross-sectional view of bench mark thruster used to infer Hall parameter.

Table 1 Current density, field, and velocity inputs for analysis

	j_y, A/cm^2	E_x, V/m	E_y, V/m	B_z, T	v_x, m/s	v_y, m/s
8kA and 16g/s	70	800	1,000	0.0192	2,359	−411
8kA and 4g/s	70	600	1,500	0.0176	4,700	−410
16kA and 16g/s	160	2,000	3,000	0.0416	4,710	−820
16kA and 4g/s	200	3,750	5,000	0.0384	10,084	−1,778
24kA and 16g/s	250	2,500	6,700	0.0624	6,970	−1,229
24kA and 4g/s	220	4,000	9,000	0.0624	23,000	−2,000

Table 2 Classically calculated and inferred Hall parameters and electrical conductivities

	Ω_{sh}	Ω	σ_0, mho/m	σ_{sh}/σ_0
8kA and 16g/s	3.8	1.6	1062	2.4(±1.0)
8kA and 4g/s	2.6	0.4	484	7.2(±2.5)
16kA and 16g/s	6.2	2.1	1188	2.9(±1.1)
16kA and 4g/s	5.9	0.4	381	16.2(±7.2)
24kA and 16g/s	5.0	0.3	390	15.5(±6.5)
24kA and 4g/s	6.8	0.2	250	31.9(±12.1)

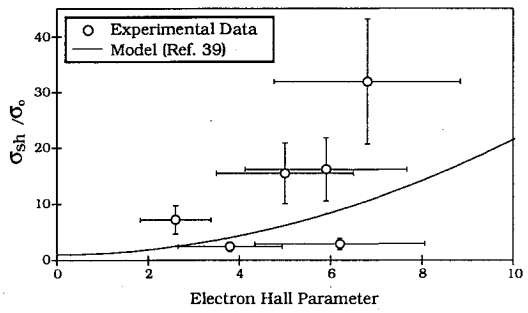

Fig. 12 Conductivity ratio vs classically calculated Hall parameter.

technique was needed to calculate conductivities consistent with the Hall parameter used in the equations above. Electrical conductivity and Hall parameter can be related by the relation

$$\Omega = (\sigma_0 m_e \omega_e / e^2 n_e) \tag{7}$$

where $\omega_e = eB/m_e$.

Table 1 lists the field and current density data used for the analysis which were obtained from Refs. 33–35. These measurements were made outside of the anode fall in a region 4 by 2 mm, centered 2 mm from the anode (cf. Fig. 11). The magnitude of exhaust velocity was estimated from the Maecker thrust law ($T \propto J^2$).[36] The plasma streaming angle (v_x/v_y) was determined from Langmuir probe measurements.[33] Neither the magnitude nor the direction (angle) of plasma streaming velocity had a perceptible influence on the outcome of the analysis.

The results of the analysis are presented in Table 2 where Ω_{sh} is obtained from Langmuir and magnetic probe data,[33,34] while Ω and σ_0 are inferred from field and current density measurements. The electrical conductivity (σ_{sh}) was calculated from the Spitzer-Härm formula for the transverse electrical resistivity[37,38]

$$\frac{1}{\sigma_{sh}} \equiv \eta_\perp = \frac{e^2\sqrt{m_e}\ \ln \Lambda}{3(2\pi)^{3/2}\varepsilon_0^2 (kT_e)^{3/2}} \tag{8}$$

Λ is given by

$$\Lambda = 9(\tfrac{4}{3})\pi n_e \lambda_e^3 \tag{9}$$

where λ_e is calculated from

$$\lambda_e = \sqrt{\frac{\varepsilon_0 k T_e}{n_e e^2}} \tag{10}$$

As Table 2 shows, the inferred plasma conductivity can be several times smaller than that calculated with Eq. (8), corroborating Lovberg's[32] suspicion that nonclassical phenomena, in some form, dictate plasma conductivity. In half of the cases studied, the inferred conductivity was over an order of magnitude smaller than the classical value. Most of the error associated with the analysis in calculating both classical and inferred conductivities results from electric field uncertainties due to the fidelity of the probe positioning system (±1 mm), the accuracy of the current density measurements in this region (20%), and the error in measuring electron number density and temperature (60 and 10%, respectively).

Figure 12 shows the ratio of classical conductivity to inferred conductivity as a function of measured electron Hall parameter. The figure also presents anomalous conductivity ratios (anomalous to classical) obtained from the microinstability model developed by Choueiri[27,39] for the case of $T_e = T_i$. As the figure shows, qualitative agreement between the model and the experimental data is exhibited, implying that instabilities near the anode lead to anomalously high resistivities. This statement is further supported by the fact that the instability which the model assumes has recently been shown to exist near the anode through analysis of Langmuir probe spectra.[40] The plasma conductivity is more than 30 times smaller than the classical value at the highest $J^2/\dot{m}$ investigated. This operating condition corresponds to that in which the largest discrepancy between anode falls determined through floating probe and heat-flux measurements is observed (cf. Fig. 5).

Summary

An array of thermocouples embedded within a modified bench mark anode, as well as floating and triple probes, were used to measure the anode heat flux and anode fall. Results from either technique are in excellent agreement with each other except at the highest level of thruster power (~7 MW). The reason for this discrepancy may be due to anode ablation and/or the fact that at high power levels, the voltage drop measured through the highly resistive plasma with floating probes may not correspond solely to the anode fall.

Argon and helium propellants were used at mass flow rates between 1–16 g/s and thruster currents between 4–25 kA. In addition, alumina insulated some 85% of the anode surface, exposing just the lip region to the discharge. Reduction of the anode's conducting surface area by a factor of six was found to have negligible effect on thruster operation. Anode power fraction with argon propellant varied from 50% at 1.9 MW to 23% at 7 MW, and with helium from 70% at 150 kW to 25% at 3.2 MW. Anode power fraction does not monotonically decrease with thruster power and is strongly dependent on mass flow rate and exhaust velocity. For helium, the anode power fraction remains constant for $J^2/\dot{m}$ above 100 kA^{2}s/g. The anode fall, which varies from 5 to 50 V for both argon and helium propellants, is by far the most significant source of anode heating. The anode heat remains constant, with argon, beyond a $J^2/\dot{m}$ of 70 kA^{2}s/g. Below this value, the anode fall increases monotonically with $J^2/\dot{m}$. For helium, however, this plateauing does not occur, and for $J^2/\dot{m}$ above 100 kA^{2}s/g the anode fall increases monotonically.

Conclusions

The electron Hall parameter, as calculated from probe measurements at the anode lip, is seen as the key scaling

parameter for the anode fall in the case of either propellant. Two possible explanations for this result have been presented: 1) the establishment of large electric fields at the anode to maintain current conduction across strong magnetic fields; and 2) the onset of microturbulence in the plasma. To investigate the latter hypothesis, electric field, magnetic field, and current density profiles measured in the vicinity of the anode were used in the generalized Ohm's law to estimate the electrical conductivity of the plasma. Results of the analysis predict conductivities in excess of 30 times lower than that calculated through classical formulas, suggesting the presence of anomalous transport.

Acknowledgments

The authors wish to thank G. Miller and D. Tregurtha for their assistance in the laboratory. This research was supported in part by NASA Contract 954997.

References

[1]Palaszewski, B., "Electric Propulsion Parameters for Manned Mars Exploration," 1989 JANNAF Propulsion Meeting, Chemical Propulsion Information Agency, Laurel, MD, May 23–25, 1989.

[2]Hack, K. J., George, J. A., Riehl, J. P., and Gilland, J. H., "Evolutionary Use of Nuclear Electric Propulsion," AIAA Space Programs and Technologies Conf., AIAA Paper 90-3821, Huntsville, AL, Sept. 25–28, 1990.

[3]Gallimore, A. D., Kelly, A. J., and Jahn, R. G., "Anode Power Deposition in Quasi-Steady MPD Thrusters," 21st International Electric Propulsion Conf., AIAA Paper 90-2668, Orlando, FL, July 18–20, 1990.

[4]Gallimore, A. D., Myers, R. M., Kelly, A. J., and Jahn, R. G., "Anode Power Deposition in an Applied-Field Segmented Anode MPD Thruster," 27th Joint Propulsion Conf., AIAA Paper 91-2343, Sacramento, CA, June 24–27, 1991.

[5]Saber, A. J., "Anode Power in a Quasi-Steady MPD Thruster," Ph.D. Dissertation, Dept. of Aerospace and Mechanical Sciences, Princeton Univ., Princeton, NJ, 1974.

[6]Myers, R. M., "Applied-Field MPD Thruster Geometry Effects," 27th Joint Propulsion Conf., AIAA Paper 91-2342, Sacramento, CA, June 24–26, 1991.

[7]Oberth, R. C., "Anode Phenomenon in High-Current Discharges," Ph.D. Dissertation, Dept. of Aerospace and Mechanical Sciences, Princeton Univ., Princeton, NJ, 1970.

[8]Saber, A. J., and Jahn, R. G., "Pulsed Electromagnetic Gas Acceleration," NASA NGLL 31-001-005 Progress Rept., July 1–Dec. 31, 1971, Dept. of Aerospace and Mechanical Sciences Semiannual Rept. 634r, Princeton Univ., Princeton, NJ, 1972.

[9]Hügel, H., "Effect of Self-Magnetic Forces on the Anode Mechanism of a High Current Discharge," *IEEE Transactions on Plasma Science*, Vol. PS-8, No. 4, 1980, pp. 437–442.

[10]Vainberg, L. I., Lyubimov, G. A., and Smolin, G. G., "High-Current Discharge Effects and Anode Damage in an End-Fire Plasma Accelerator," *Soviet Physics—Technical Physics* (translation of *Zhurnal Teknicheskoi Fiziki*), Vol. 23, No. 4, 1978, pp. 439–443.

[11]Eckert, E. R. G., and Pfender, E., *Advances in Heat Transfer*, edited by J. P. Harnet, and T. F. Irvine, Jr., Vol. 2, Academic Press, New York, 1967, pp. 229–316.

[12]Subramaniam, V. V., and Lawless, J. L., "Electrode-Adjacent Boundary Layer Flow in Magnetoplasmadynamic Thrusters," Carnegie-Mellon Univ., Draft Rept., Pittsburgh, PA, 1987.

[13]Randolph, T. M., personal communication, Princeton Univ., Princeton, NJ, Aug. 1991.

[14]Gallimore, A. D., Dept. of Mechanical and Aerospace Engineering, Rept. 1776.29, Princeton Univ., Princeton, NJ, Jan.–Feb. 1991.

[15]Laframboise, J., "Theory of Cylindrical and Spherical Probes in a Collisionless Plasma at Rest," *Rarefied Gas Dynamics*, edited by J. H. deLeeuw, Vol. 2, Academic Press, New York, 1966, p. 22.

[16]Peterson, E. W., and Talbot, L., "Collisionless Electrostatic Single-Probe Parameters by Means of Triple Probe," *AIAA Journal*, Vol. 8, No. 12, 1970, pp. 2215–2219.

[17]Tilley, D., Kelly, A. J., and Jahn, R. G., "The Application of the Triple Probe Method to MPD Thruster Plumes," 21st International Electric Propulsion Conf., AIAA Paper 90-2667, Orlando, FL, July 18–20, 1990.

[18]Karkosak, J. J., and Hoffman, M. A., "Electrode Drops and Current Distribution in an MGD Channel," *AIAA Journal*, Vol. 3, No. 6, 1965, pp. 1198–1200.

[19]Kisov, A. Ya., Morozov, A. I., and Tilinin, G. N., "Distribution of Potential in a Quasistationary Coaxial Plasma Injector," *Soviet Physics—Technical Physics* (translation of *Zhurnal Teknicheskoi Fiziki*), Vol. 13, No. 6, 1968, pp. 467–472.

[20]Morozov, A. I., and Solov'ev, L. S., "Plane Flows of Ideally Conducting Compressible Fluids with Hall Effect Considered," *Soviet Physics—Technical Physics* (translation of *Zhurnal Teknicheskoi Fiziki*), Vol. 9. No. 7, 1965, pp. 889–897.

[21]Jahn, R. G., *Physics of Electric Propulsion*, McGraw-Hill, New York, 1968.

[22]Aref'ev, V. I., "Current-Driven Instabilities in a Strongly Inhomogeneous Plasma. I," *Soviet Physics—Technical Physics* (translation of *Zhurnal Teknicheskoi Fiziki*), Vol. 17, No. 7, 1973, pp. 1095–1102.

[23]Aref'ev, V. I., "Current-Driven Instabilities in a Strongly Inhomogeneous Plasma. II." *Soviet Physics—Technical Physics* (translation of *Zhurnal Teknicheskoi Fiziki*), Vol. 17, No. 7, 1973, pp. 1103–1107.

[24]Aref'ev, V. I., "Plasma Acceleration in Crossed Electric and Magnetic Fields," *Soviet Physics—Technical Physics* (translation of *Zhurnal Teknicheskoi Fiziki*), Vol. 19, No. 4, 1974, pp. 446–454.

[25]Aref'ev, V. I., and Kirdyashev, K. P., "Excitation of High-Frequency Waves in a Plasma with an Accelerating Hall Sheath," *Soviet Physics—Technical Physics* (translation of *Zhurnal Teknicheskoi Fiziki*), Vol. 20, No. 3, 1975, pp. 330–334.

[26]Hoskins, W. A., "Asymmetric Discharge Patterns in the MPD Thruster," M.S. Thesis, Dept. of Mechanical and Aerospace Engineering, Princeton Univ., Princeton, NJ, 1990.

[27]Choueiri, E. Y., "Electron-Ion Streaming Instabilities of an Electromagnetically Accelerated Plasma," Ph.D. Dissertation, Dept. of Mechanical and Aerospace Engineering, Princeton Univ., Princeton, NJ, 1991.

[28]Auweter-Kurtz, M., Kurtz, H. L., Merke, W. D., Scharde, H. O., and Christian-Sleziona, P., "Self Field MPD Thruster Investigation," FY'88 Final Rept. (unpublished), Inst. für Raumfahrtsysteme, IRS-88-P-10, Univ. Stuttgart, Stuttgart, Germany, 1988.

[29]Auweter-Kurtz, M., Kurtz, H. L., Merke, W. D., Scharde, H. O., Christian-Sleziona, P., and Wegmann, T., "High Power Steady State MPD Thruster," FY'89 Final Rept. (unpublished), Inst. für Raumfahrtsysteme, IRS-90-P4, Univ. Stuttgart, Stuttgart, Germany, 1990.

[30]Kuriki, K., and Iida, H., "Spectrum Analysis of Instabilities in MPD Thruster," 17th International Electric Propulsion Conf., Japan Society for Aeronautical and Space Sciences, IEPC 84-28, Tokyo, 1984.

[31]Tilley, D. L., "An Investigation of Microinstabilities in a kW Level Self-Field MPD Thruster," M.S. Thesis, Dept. of Mechanical and Aerospace Engineering, Princeton Univ., Princeton, NJ, 1991.

[32]Lovberg, R. H., "Plasma Problems in Electric Propulsion," *Methods of Experimental Physics, Plasma Physics*, edited by R. H. Lovberg, and H. R. Griem, Vol. 9, Academic Press, New York, 1971, Pt. B, Chap. 16.

[33]Gallimore, A. D., Dept. of Mechanical and Aerospace Engineering, Rept. 1776.24, Princeton Univ., Princeton, NJ, March–April 1990.

[34]Gallimore, A. D., Dept. of Mechanical and Aerospace Engineering, Rept. 1776.19, Princeton Univ., Princeton, NJ, May–June 1989.

[35]Gallimore, A. D., Dept. of Mechanical and Aerospace Engineering, Rept. 1776.25, Princeton Univ., Princeton, NJ, May–June 1990.

[36]Choueiri, E. Y., Dept. of Mechanical and Aerospace Engineering, Rept. 1776.14, Princeton Univ., Princeton, NJ, March 1987.

[37]Chen, F. F., "Introduction to Plasma Physics and Controlled Fusion," *Plasma Physics*, Vol. 1, 2nd ed., Plenum Press, New York, 1984, pp. 178–183.

[38]Spitzer, L., Jr., *Physics of Fully Ionized Gases*, Wiley, New York, 1962, pp. 138, 139.

[39]Caldo, G., Choueiri, E. Y., Kelly, A. J., and Jahn, R. G., "An MPD Code with Anomalous Transport," 22nd International Electric Propulsion Conf., AIAA Paper 91-102, Viareggio, Italy, Oct. 14–17, 1991.

[40]Diamant, K. D., Dept. of Mechanical and Aerospace Engineering, Rept. 1776.35, Princeton Univ., Princeton, NJ, Jan.–Feb. 1992.